C. R. Acad. Sci. Paris, Ser. I 355 (2017) 1026–1036

Contents lists available at ScienceDirect

C. R. Acad. Sci. Paris, Ser. I

www.sciencedirect.com

Statistics/Theory of signals

An improved SSA forecasting result based on a filtered recurrent forecasting algorithm

Un algorithme de prévision SSA amélioré, reposant sur des séries filtrées

Hossein Hassani [a], Mahdi Kalantari [b], Masoud Yarmohammadi [b]

[a] *Research Institute of Energy Management and Planning, University of Tehran, No. 13, Ghods St., Enghelab Ave., Tehran, Iran*
[b] *Department of Statistics, Payame Noor University, 19395-4697, Tehran, Iran*

ARTICLE INFO

Article history:
Received 6 May 2017
Accepted after revision 11 September 2017
Available online 28 September 2017

Presented by the Editorial Board

ABSTRACT

The Singular Spectrum Analysis (SSA) technique is a non-parametric powerful method in the field of time series analysis whose popularity has increased in recent years owing to its widespread applications. Recurrent forecasting is one of the important forecasting methods in SSA. In this paper, the forecasting accuracy of recurrent forecasts is improved via the introduction of a new recurrent forecasting algorithm. In the novel approach, the recurrent coefficients are generated from the filtered series which has less noise and thus enables one to achieve the better forecasts. The performance of the new method has been compared with the established recurrent forecasting method. The comparison involves applications to various real and simulated time series. The obtained results confirm that the new approach can provide more accurate forecasts.

RÉSUMÉ

La technique d'analyse du spectre singulier (SSA) est une méthode puissante et non paramétrique dans le domaine de l'analyse des séries temporelles. Elle connaît depuis ces dernières années une popularité croissante en raison de son large éventail d'applications. La prévision récurrente est l'une des plus importantes méthodes de prévision en SSA. Dans ce texte, nous améliorons la précision de ces prévisions récurrentes en introduisant un nouvel algorithme. Dans notre approche, les coefficients récurrents sont engendrés à partir d'une série filtrée qui a un bruit moindre, ce qui permet d'obtenir de meilleures prévisions. Nous comparons cette nouvelle méthode avec celle établie, en la testant sur des applications à diverses séries temporelles, réelles ou simulées. Les résultats confirment que la nouvelle méthode produit des prévisions plus précises.

E-mail addresses: kalantarimahdi@pnu.ac.ir (M. Kalantari), masyar@pnu.ac.ir (M. Yarmohammadi).

http://dx.doi.org/10.1016/j.crma.2017.09.004
1631-073X/

1. Introduction

The field of time series analysis and forecasting is of utmost importance to all industries across the globe as a result of the increasing uncertainty that we are faced with. This is because forecasting models have the capability of enabling better decision making, planning, and risk management. However, the success of such efforts depend largely on the nature of the forecasting technique (i.e. parametric or non-parametric), accuracy of the forecasts (as measured by loss functions), and the ability to predict the correct direction of change. Accordingly, there are continuous attempts at improving forecasting algorithms in order to meet these criteria and improve upon them. Whilst it is not the intention of this paper to review all such work, the interested reader is referred to a few successful examples that can be found in [8,16,17].

Instead, the focus of this paper revolves around a non-parametric technique known as Singular Spectrum Analysis (SSA), which has both filtering and forecasting capabilities that can be exploited in either an univariate or a multivariate form [20]. The model-free nature of SSA is advantageous, as the parametric assumptions relating to normality and stationarity, which are unlikely to hold in the real world, are irrelevant when modeling and forecasting using SSA. In brief, the SSA technique initially filters a time series, and then reconstructs a less noisy series, which is used for forecasting. This is yet another advantage of SSA over the classical time series methods as decomposition of a time series enables one to obtain a richer understanding of the underlying variation in a given data set and also helps achieve better forecasts as most (if not all) of the randomness is filtered out. Recently, there has been an augment in the popularity of SSA as a forecasting method, as evidenced by its wide ranging applications, see, for example, [1,2,5,6,13–15,18,19,21,22].

The introduction of SSA dates back to the work by Broomhead and King [3,4] in 1986. Since then, there has been various attempts at improving the decomposition, reconstruction, and forecasting via SSA (see, for example, [11]). The increasing applications of SSA in the recent past suggests that it has now developed into a technique that is recognized as a powerful tool for time series analysis and forecasting. This has resulted in additional attempts at further understanding and improving the theory underlying SSA. For example, in [12] the authors evaluated the impact of outliers on SSA, and in [14] the authors proposed an automated and optimized SSA forecasting algorithm that enables users who are not conversant with the complex theory underlying SSA to exploit the technique for forecasting. This paper adds to the developments in the field of SSA, as it seeks to improve its forecasting performance.

The univariate SSA process has two forecasting variations known as recurrent SSA (SSA-R) and Vector SSA (SSA-V) [20]. The SSA-V approach, in particular, has been widely adopted in recent studies [14,22], whilst the application of SSA-R has remained minimal. This is not only because SSA-V has shown better performance in the presence of outliers [12], but also because SSA-R forecasts have failed to outperform SSA-V in most instances, see for example [14] and references therein. Having identified the need for improving the SSA-R forecasting approach, and motivated by the negative perception towards the use of SSA-R, this paper aims to improve upon the forecasting capability of the basic SSA-R process in [9], and to develop a novel SSA-R forecasting algorithm that can provide comparatively more accurate forecasts. In brief, the novel approach considers generating SSA-R coefficients from the filtered series as opposed to the process followed in the basic SSA-R process in [9], whereby the coefficients are generated from the noisy time series.

The remainder of this paper is organized as follows. Section 2 presents a review of SSA and the recurrent forecasting algorithm. The novel SSA-R forecasting approach is presented in Section 3 and in Section 4, the performance of the new method is compared with the established SSA-R approach by applying it to simulated and real time series data. Section concludes the paper.

2. Review of SSA

The theory underlying basic SSA has been explained in detail in [20]. In brief, the SSA procedure consists of two complementary stages: *decomposition* and *reconstruction*, each with two separate steps. At the first stage, the series is decomposed into several components in order to enable signal extraction and noise reduction. At the second stage, a less noisy series is reconstructed, which can be used for forecasting new data points. The basic SSA process is concisely presented below, and in doing so we mainly follow [10,14].

Stage 1: decomposition (embedding & singular value decomposition)

In the embedding step, the one-dimensional time series $Y_N = \{y_1, \ldots, y_N\}$ is mapped into the multi-dimensional series $X_1, \ldots, X_K$ with vectors $X_i = (y_i, \ldots, y_{i+L-1})^{\mathrm{T}} \in \mathbf{R}^L$, where $K = N - L + 1$. The vectors X_i are called *L-lagged vectors*. The single choice of this step is the window length L, which is an integer such that $2 \leq L \leq N/2$. The output of the embedding step is the trajectory matrix $\mathbf{X}$, which is also a Hankel matrix and takes the following form:

$$\mathbf{X} = [X_1 : \cdots : X_K] = (x_{ij})_{i,j=1}^{L,K} = \begin{pmatrix} y_1 & y_2 & y_3 & \cdots & y_K \\ y_2 & y_3 & y_4 & \cdots & y_{K+1} \\ \vdots & \vdots & \vdots & \ddots & \vdots \\ y_L & y_{L+1} & y_{L+2} & \cdots & y_N \end{pmatrix}.$$

The singular value decomposition (SVD) step is aimed at representing the trajectory matrix $\mathbf{X}$ as a sum of rank-one elementary matrices. The eigenvalues of $\mathbf{X}\mathbf{X}^{\mathrm{T}}$ are denoted by $\lambda_1, \ldots, \lambda_L$, in decreasing order of magnitude ($\lambda_1 \geq \cdots \geq \lambda_L \geq 0$),

and by $U_1, \ldots, U_L$, the eigenvectors of the matrix $\mathbf{X}\mathbf{X}^{\mathrm{T}}$ corresponding to these eigenvalues. If $d = \max\{i, \text{ such that } \lambda_i > 0\} = \operatorname{rank}\mathbf{X}$, then the SVD of the trajectory matrix can be written as $\mathbf{X} = \mathbf{X}_1 + \cdots + \mathbf{X}_d$, where $\mathbf{X}_i = \sqrt{\lambda_i} U_i V_i^{\mathrm{T}}$ and $V_i = \mathbf{X}^{\mathrm{T}} U_i / \sqrt{\lambda_i}$ $(i = 1, \ldots, d)$.

Stage 2: reconstruction (grouping & diagonal averaging)

The grouping step splits the elementary matrices $\mathbf{X}_i$ into several groups and sums the matrices within each group. If a group of indices $i_1, \ldots, i_p$ is denoted by $I = \{i_1, \ldots, i_p\}$, then the matrix $\mathbf{X}_I$ corresponding to the group I is defined as $\mathbf{X}_I = \mathbf{X}_{i_1} + \cdots + \mathbf{X}_{i_p}$. Having the SVD of $\mathbf{X}$, the split of the set of indices $\{1, \ldots, d\}$ into the disjoint subsets $I_1, \ldots, I_m$ corresponds to the following representation:

$$\mathbf{X} = \mathbf{X}_{I_1} + \cdots + \mathbf{X}_{I_m}. \tag{1}$$

Diagonal averaging is a process that transforms each matrix $\mathbf{X}_{I_j}$ of the grouped decomposition (1) into a Hankel matrix so that these can subsequently be converted into a time series, which is an additive component of the initial series Y_N. Assume that z_{ij} stands for an element of a matrix $\mathbf{Z}$, then the k-th term of the resulting series is obtained by averaging z_{ij} over all i, j, such that $i + j = k + 2$. This procedure is also known as the Hankelization of the matrix $\mathbf{Z}$. The output of the Hankelization of a matrix $\mathbf{Z}$ is the Hankel matrix $\mathcal{H}\mathbf{Z}$, which is the trajectory matrix corresponding to the series obtained as a result of the diagonal averaging. In its turn, the Hankel matrix $\mathcal{H}\mathbf{Z}$ uniquely defines the series by relating the value in the anti-diagonals to the values in the series. By applying the Hankelization procedure to all matrix components of (1), this expansion is obtained: $\mathbf{X} = \widetilde{\mathbf{X}}_{I_1} + \cdots + \widetilde{\mathbf{X}}_{I_m}$, where $\widetilde{\mathbf{X}}_{I_j} = \mathcal{H}\mathbf{X}_{I_j}$, $j = 1, \ldots, m$. This is equivalent to the decomposition of the initial series $Y_N = \{y_1, \ldots, y_N\}$ into a sum of m series: $y_t = \sum_{k=1}^{m} \widetilde{y}_t^{(k)} (t = 1, \ldots, N)$, where $\widetilde{Y}_N^{(k)} = \{\widetilde{y}_1^{(k)}, \ldots, \widetilde{y}_N^{(k)}\}$ corresponds to the matrix $\widetilde{\mathbf{X}}_{I_k}$.

Following the decomposition and reconstruction stages, which are crucial for signal extraction and noise filtering, the technique also has the capability of generating forecasts using the filtered time series. In what follows, forecasting with SSA is discussed at length focusing mainly on SSA-R. The reader interested in the process underlying SSA-V is referred to [20].

2.1. Recurrent SSA forecasting (SSA-R)

The basic requirement to be able to perform SSA forecasting is that the series satisfies a linear recurrent relation (LRR). The time series $Y_N = \{y_1, \ldots, y_N\}$ satisfies an LRR of order d if there exist the coefficients $a_1, \ldots, a_d$ such that:

$$y_{i+d} = \sum_{k=1}^{d} a_k y_{i+d-k}, \quad 1 \le i \le N - d, \quad a_d \neq 0, \quad d < N.$$

The series governed by LRRs admits natural recurrent continuation, since each term of such a series is a linear combination of several preceding terms. Similar to an autoregressive model, SSA forecasting is based on the multiplication of a weight of the previous observation. This weight is obtained based on the eigenvector.

An important advantage of SSA is that it allows us to produce forecasts for either the individual components of the series or the reconstructed series itself. Suppose that I is the chosen set of eigentriples from the grouping step. In trend forecasting, I is the trend group and in harmonic components forecasting, I corresponds to harmonic groups. To produce forecasts for reconstructed series (signal forecasting), the first r eigentriples can be selected.

Let I be the chosen set of eigentriples, $U_i \in \mathbf{R}^L$ and $i \in I$ be the corresponding eigenvectors, $\underline{U_i} \in \mathbf{R}^{L-1}$ be the vector consisting of the first $L - 1$ components of the vector U_i, π_i be the last component of the vector U_i, $\nu^2 = \sum_{i \in I} \pi_i^2$, and $\widetilde{Y}_N = \{\widetilde{y}_1, \ldots, \widetilde{y}_N\}$ be the series reconstructed by I. Denote by $\mathcal{L} \subset \mathbf{R}^L$ the linear space spanned by the vectors $U_i, i \in I$; i.e. $\mathcal{L} = \operatorname{span}(U_i, i \in I)$. Note that the set $\{U_i, i \in I\}$ is an orthonormal basis in $\mathcal{L}$. It is assumed that $e_L \notin \mathcal{L}$, where $e_L = (0, 0, \ldots, 1)^{\mathrm{T}} \in \mathbf{R}^L$; in other terms, $\mathcal{L}$ is not a *vertical* space. Since $e_L \notin \mathcal{L}$, $\nu^2 < 1$, it can be proved that the last component z_L of any vector $Z = (z_1, \ldots, z_L)^{\mathrm{T}} \in \mathcal{L}$ is a linear combination of the first components $z_1, \ldots, z_{L-1}$, i.e. $z_L = a_1 z_{L-1} + \cdots + a_{L-1} z_1$, (see [9]) where the vector $R = (a_{L-1}, \ldots, a_1)^{\mathrm{T}}$ is defined as:

$$R = \frac{1}{1 - \nu^2} \sum_{i \in I} \pi_i \underline{U_i}. \tag{2}$$

The SSA-R forecasting algorithm can be presented as follows.

1. The time series $Z_{N+h} = \{z_1, \ldots, z_{N+h}\}$ is defined by

$$z_i = \begin{cases} \widetilde{y}_i & \text{for } i = 1, \ldots, N \\ \sum_{j=1}^{L-1} a_j z_{i-j} & \text{for } i = N+1, \ldots, N+h. \end{cases} \tag{3}$$

2. The numbers $z_{N+1}, \ldots, z_{N+h}$ are the h step ahead recurrent forecasts.

Therefore, it is clear that SSA-R forecasting is performed by the direct use of the LRR with coefficients $\{a_j, j = 1, \ldots, L-1\}$ as defined in (2). In what follows, the coefficients $\{a_j, j = 1, \ldots, L-1\}$ in (2) will be called *SSA-R coefficients*.

3. New SSA-R forecasting algorithm

Consider a noisy time series y_t that is the sum of two components, a noise-free series (signal) and noise. On the other hand, we have:

$$y_t = s_t + n_t, \quad t = 1, \ldots, N, \tag{4}$$

where s_t and n_t represent the signal and noise components, respectively. It is evident from Relation (4) that:

$$\mathbf{X} = \mathbf{S} + \mathbf{N}, \tag{5}$$

where $\mathbf{S}$ and $\mathbf{N}$ represent $L \times K$ trajectory matrices of the signal and the noise components, respectively.

For any time series with a fixed window length L, there are $L-1$, SSA-R coefficients $a_1, \ldots, a_{L-1}$. In theory, if it is assumed that a time series y_t is not contaminated with noise, i.e. $y_t = s_t$, the exact values of SSA-R coefficients can be obtained. However, in reality, y_t is contaminated with noise, and therefore the SSA-R coefficients, which are computed based on noisy y_t, will differ from the exact values. This is because, as per (2), SSA-R coefficients are built on U_i, $i \in I$ and U_is are not noise free. Recall that U_is are eigenvectors of $\mathbf{X}\mathbf{X}^{\mathrm{T}}$ and the trajectory matrix $\mathbf{X}$ is contaminated with noise according to (5).

It is clear from Relation (3) that SSA-R coefficients play a fundamental role in SSA-R forecasting and using inadequate coefficients results in low-accuracy predictions. Since the reconstructed series includes less noise, it seems that SSA-R coefficients obtained via the reconstructed series can improve SSA-R forecasting. This simple, yet lucrative idea leads us to a new SSA-R forecasting algorithm whereby its coefficients are computed from the reconstructed series. From this point forward, SSA-R is used to identify the recurrent forecasting algorithm based on the original series, whereas the SSA-R forecasting algorithm based on the reconstructed series is referred to as *reconstructed SSA-R*.

Let I be the chosen set of eigentriples, $\widetilde{Y}_N = \{\widetilde{y}_1, \ldots, \widetilde{y}_N\}$ be the series reconstructed by I, $\widetilde{\mathbf{X}}$ be the trajectory matrix of reconstructed series, $\widetilde{\lambda}_1, \ldots, \widetilde{\lambda}_L$ be the eigenvalues of $\widetilde{\mathbf{X}}\widetilde{\mathbf{X}}^{\mathrm{T}}$ in decreasing order of magnitude ($\widetilde{\lambda}_1 \geq \cdots \geq \widetilde{\lambda}_L \geq 0$) and $\widetilde{U}_1, \ldots, \widetilde{U}_L$ be the corresponding eigenvectors. The Reconstructed SSA-R coefficients can then be calculated as follows:

$$\widetilde{R} = (\widetilde{a}_{L-1}, \ldots, \widetilde{a}_1)^{\mathrm{T}} = \frac{1}{1-\widetilde{\nu}^2} \sum_{i \in I} \widetilde{\pi}_i \underline{\widetilde{U}_i}, \tag{6}$$

where $\underline{\widetilde{U}_i}$ is the vector consisting of the first $L-1$ components of the vector $\widetilde{U}_i$, $\widetilde{\pi}_i$ is the last component of the vector $\widetilde{U}_i$ and $\widetilde{\nu}^2 = \sum_{i \in I} \widetilde{\pi}_i^2$. The reconstructed SSA-R forecasting algorithm can be presented as follows.

1. The time series $Z_{N+h} = \{z_1, \ldots, z_{N+h}\}$ is defined by

$$z_i = \begin{cases} \widetilde{\widetilde{y}}_i & \text{for } i = 1, \ldots, N \\ \sum_{j=1}^{L-1} \widetilde{a}_j z_{i-j} & \text{for } i = N+1, \ldots, N+h. \end{cases} \tag{7}$$

2. The numbers $z_{N+1}, \ldots, z_{N+h}$ are the h step ahead reconstructed SSA-R forecasts.

Where $\widetilde{\widetilde{Y}}_N = \{\widetilde{\widetilde{y}}_1, \ldots, \widetilde{\widetilde{y}}_N\}$ is the doubly reconstructed series.

4. Empirical results

In this section, the performance of SSA-R and reconstructed SSA-R forecasting algorithms are evaluated by applying them to simulated time series and real data. The series is split into two sets: a training sample and a test sample. The training sample is used to produce SSA forecasts. The accuracy of forecasting results are measured using the widely used metric, root mean squared error (RMSE). The following RMSE ratio is used for comparing the established (SSA-R) and the newly proposed Reconstructed SSA-R forecasting algorithms:

$$RRMSE_h = \frac{\left(\sum_{t=m}^{m+n-h} (y_{t+h} - \hat{y}_{t+h|t})^2\right)^{1/2}}{\left(\sum_{t=m}^{m+n-h} (y_{t+h} - \hat{\hat{y}}_{t+h|t})^2\right)^{1/2}},$$

where m is the length of the training sample, n is the length of the test sample, h is the length of the forecast horizon, $\hat{y}_{t+h|t}$ is the h-step ahead forecast obtained by reconstructed SSA-R and $\hat{\hat{y}}_{t+h|t}$ is the h-step ahead forecast obtained by SSA-R. If the $RRMSE_h < 1$, then reconstructed SSA-R outperforms SSA-R at horizon h. Alternatively, when $RRMSE_h > 1$, it would indicate that the performance of reconstructed SSA-R forecasting is worse than that of the original SSA-R forecasting. In order to enable better comparison, a dashed horizontal line $y = 1$ is added to all RRMSE figures.

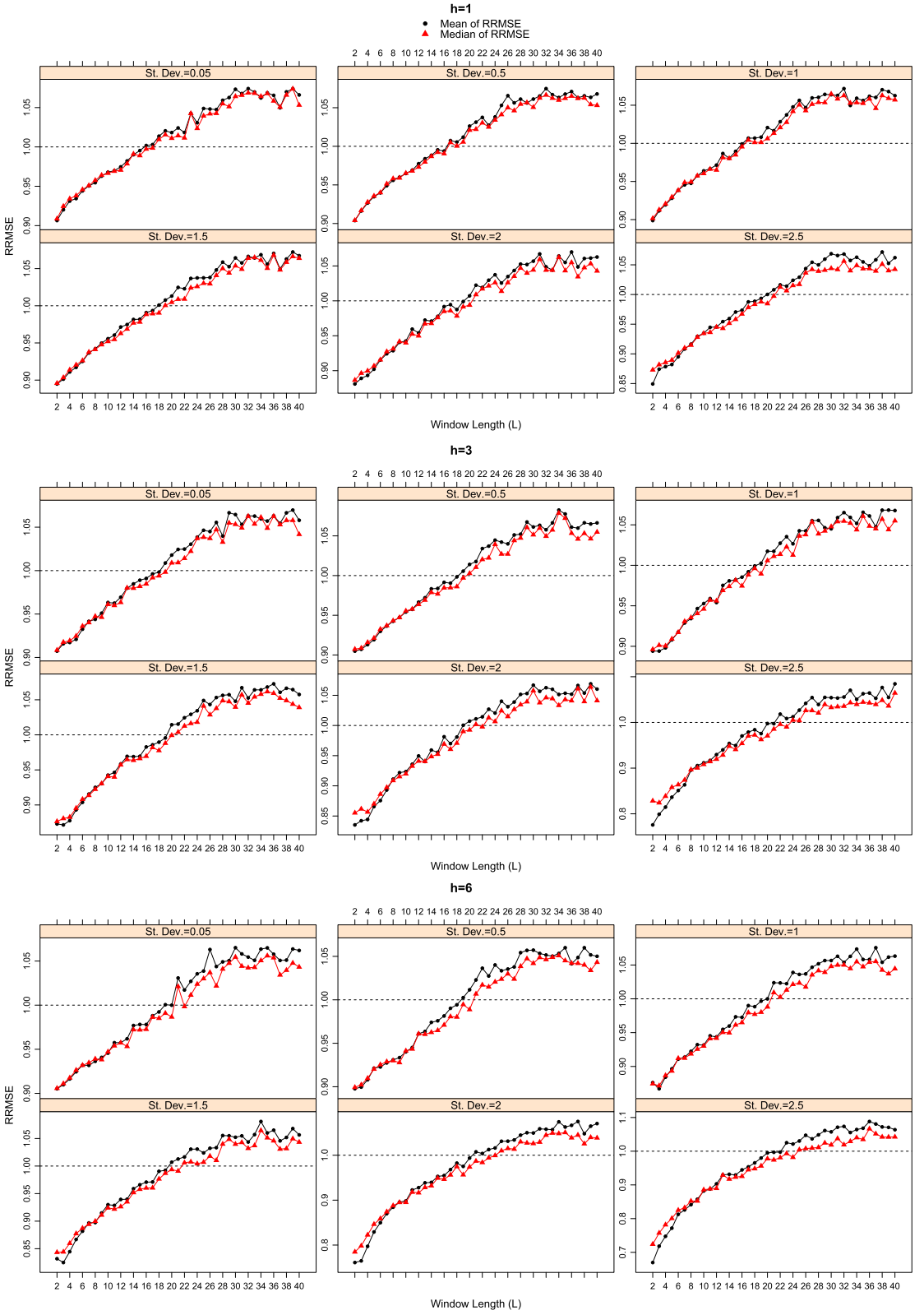

Fig. 1. RRMSE for exponential series ($h = 1, 3, 6$).

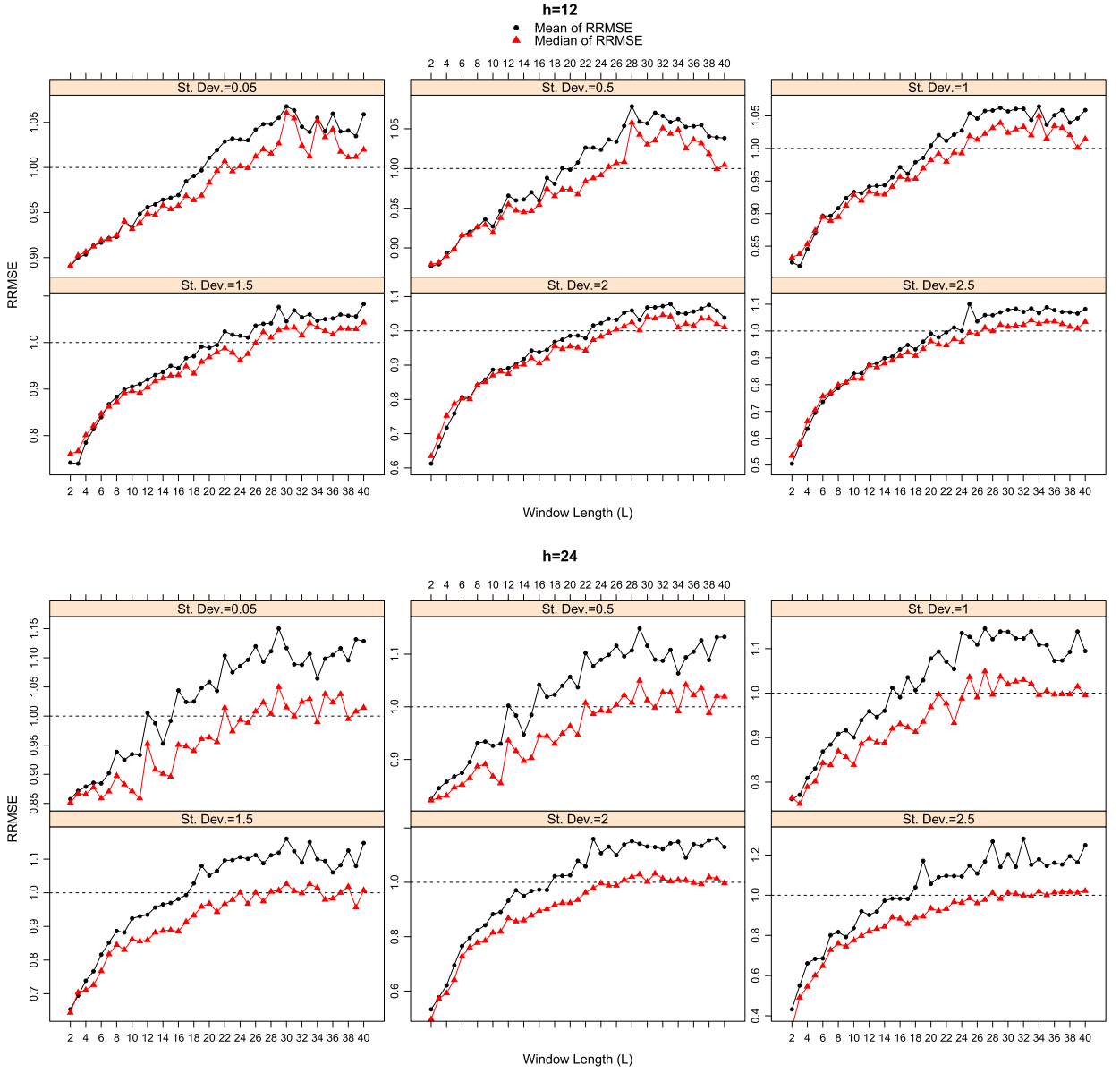

Fig. 2. RRMSE for exponential series ($h = 12, 24$).

4.1. Simulation study

In the following simulated series, 100 data points are generated and the normally distributed noise is added to each point of the signal. The first 70 observations were considered as the training sample ($m = 70$), and the rest as the test sample ($n = 30$). The number of leading eigenvalues for reconstruction and forecasting (r) were selected according to the rank of the corresponding trajectory matrix. The simulation was repeated 1000 times and the mean and the median of RRMSEs were calculated.

Example 4.1. Consider the exponential series:

$$y_t = \exp(0.01t) + n_t, \quad t = 1, 2, \ldots, 100,$$

where n_t is the normally distributed noise series. The first eigenvalue was selected for forecasting ($r = 1$). Figs. 1 and 2 show the RRMSE for 1, 3, 6, 12, and 24 forecast horizons. For each value of h, different values of the standard deviation of noise series have been used. As can be seen in these figures, the reconstructed SSA-R forecasting method outperforms SSA-R for lower values of the window length (L) up to approximately 20. Note that this result is satisfied for all forecast horizons

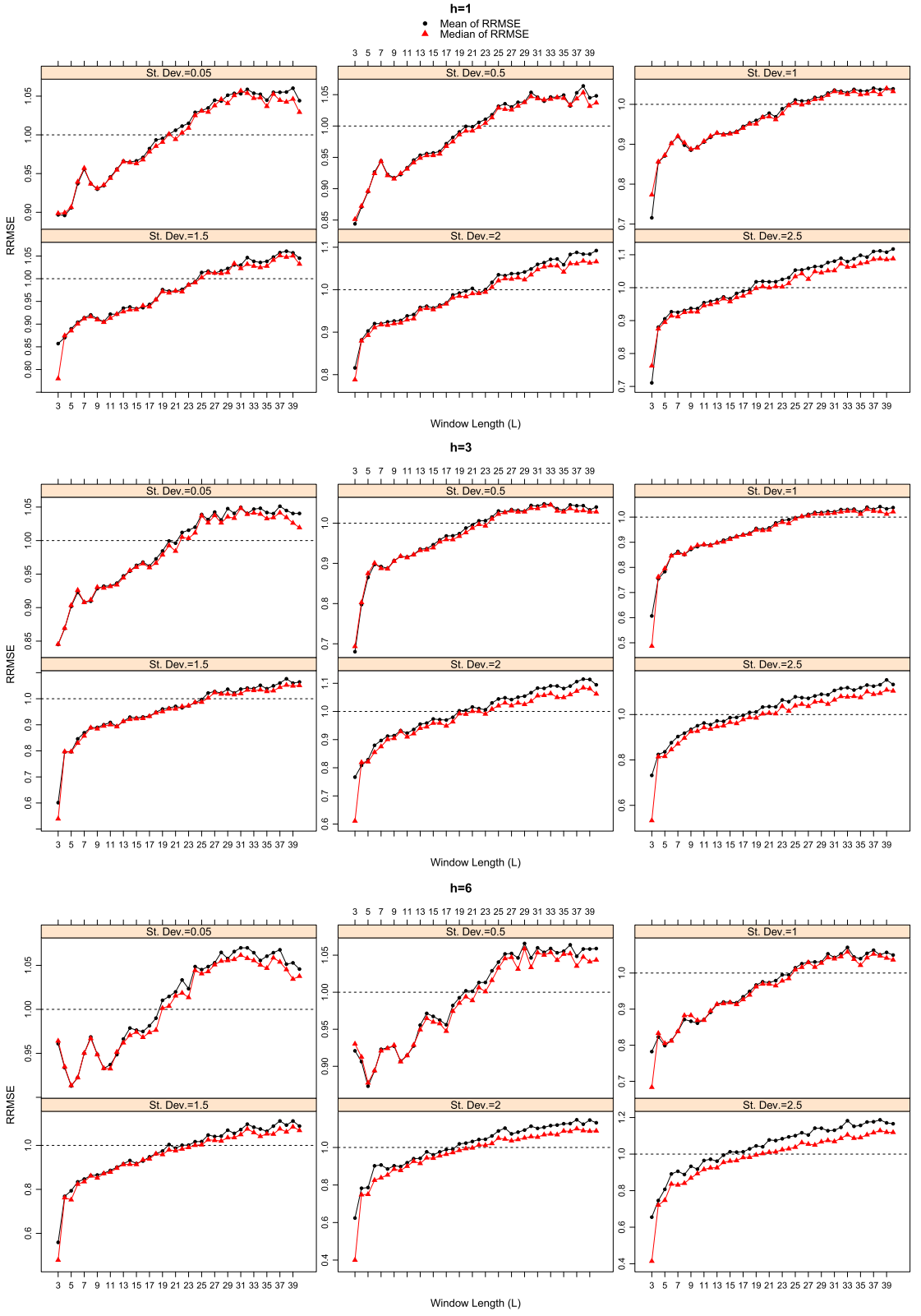

Fig. 3. RRMSE for sine series ($h = 1, 3, 6$).

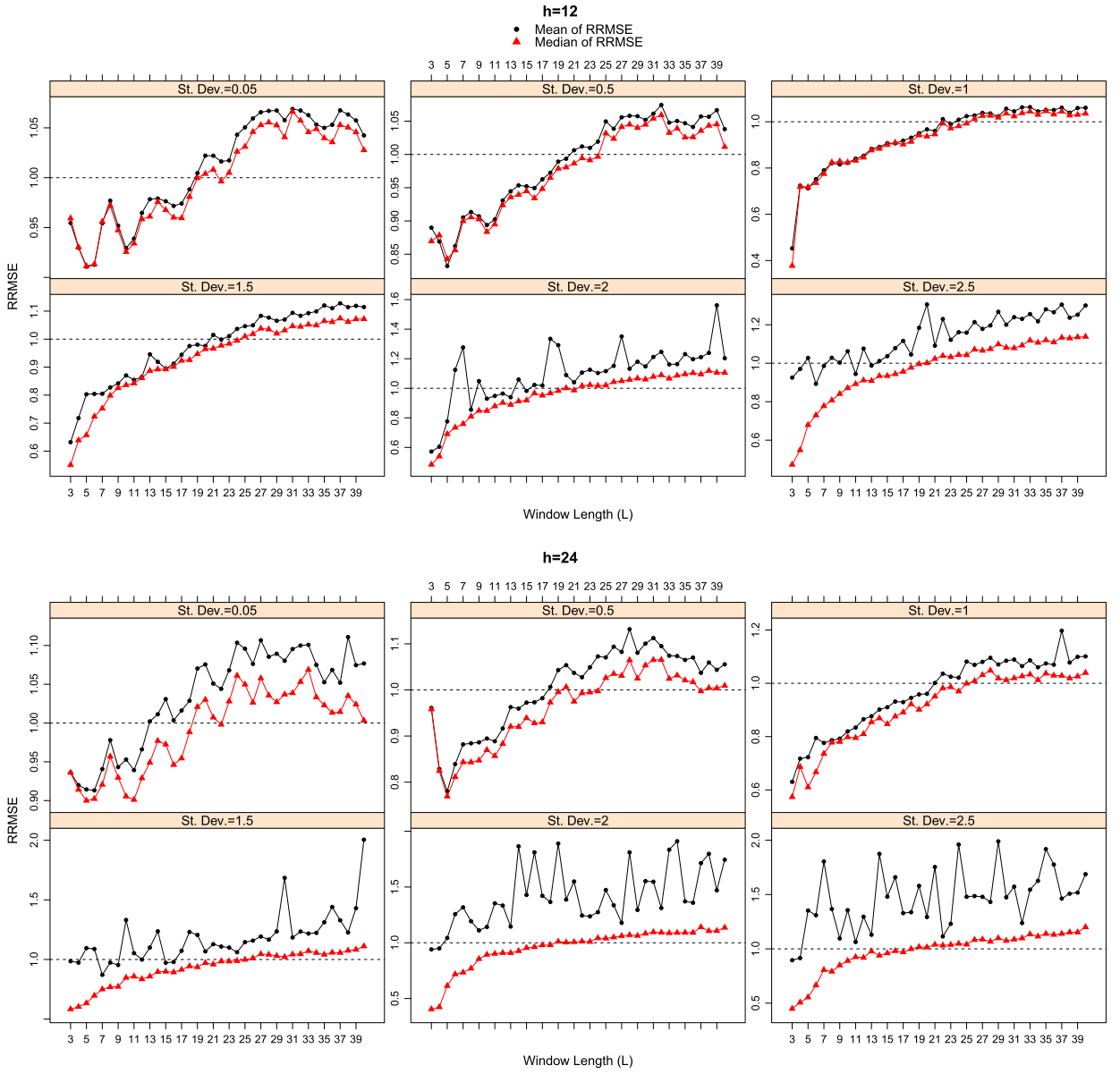

Fig. 4. RRMSE for sine series ($h = 12, 24$).

and different values of the standard deviation of noise series. Another interesting point is that the difference between the mean and the median of RRMSEs increase as h takes a larger value, especially when $h = 24$. Because the median of RRMSEs is less than the mean of the latter for each value of the standard deviation and each L, it can be concluded that the right tail weight of the distribution of RRMSE becomes heavier with h.

Example 4.2. As a second example, consider the sine series:

$$y_t = \sin(\pi t/6) + n_t, \quad t = 1, 2, \ldots, 100,$$

where n_t is the normally distributed noise series. The first two eigenvalues were selected for forecasting ($r = 2$). Figs. 3–4 show the RRMSE for 1, 3, 6, 12, and 24 forecast horizons. In a similar fashion to Example 4.1, different values of the standard deviation of noise series have been used for each value of h, and it can be concluded from these figures that the reconstructed SSA-R forecasting method outperforms SSA-R for lower values of the window length (L) up to approximately 20. It is noteworthy that this result holds for all forecast horizons and different values of standard deviation of noise series. Also, similar to simulated exponential series, the right skewness of distribution of RRMSE increases as h becomes greater.

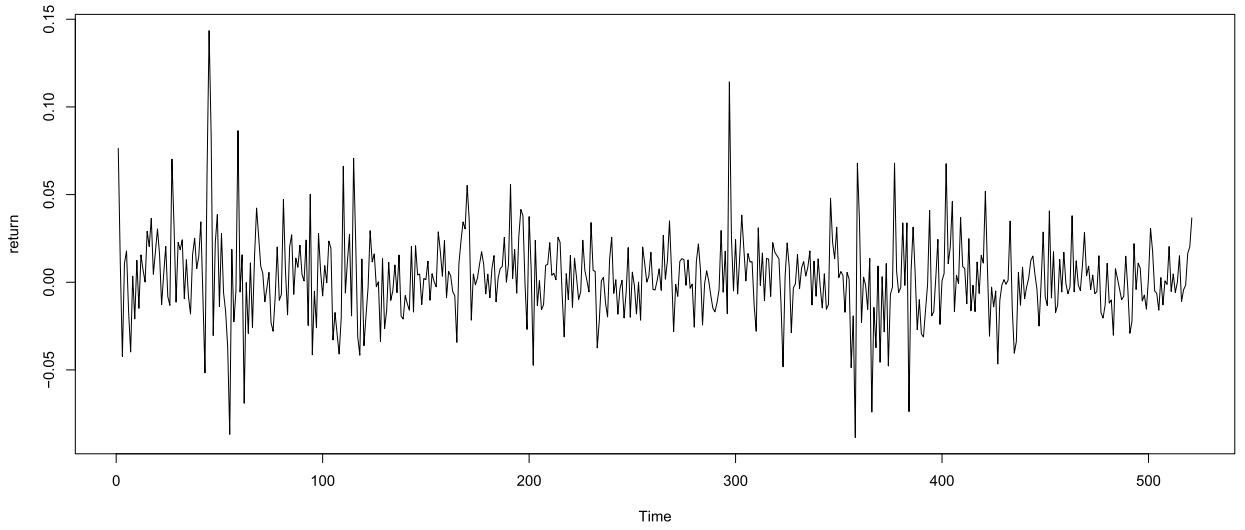

Fig. 5. Time series plot of Google series.

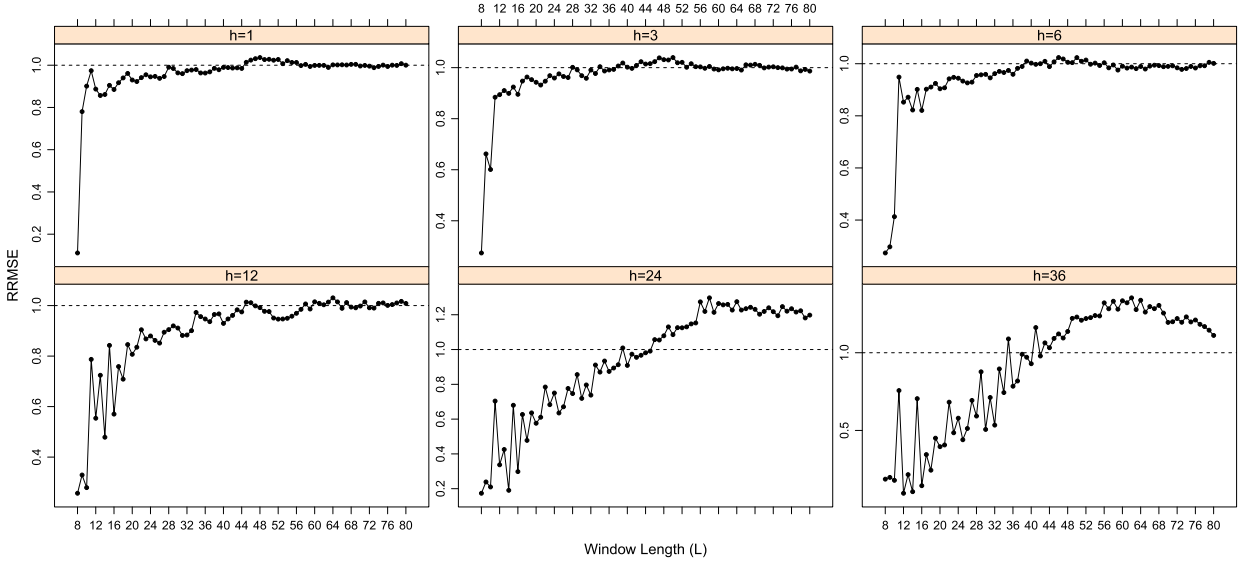

Fig. 6. RRMSE for Google series.

As can be seen for the case of $h = 12$ and 24, the fluctuation of mean of RRMSEs is greater than the fluctuation of median of RRMSEs for large values of the standard deviation.

4.2. Real data

In this subsection, the efficiency of SSA-R and reconstructed SSA-R forecasting algorithms are compared using real data.

Example 4.3. As the first real data, we consider the daily returns of Google stock from August 14, 2004 to September 13, 2006. This time series includes a total of 521 observations presented in [7]. Fig. 5 depicts the time series plot of these data.

In Fig. 6, the RRMSE for 1, 3, 6, 12, 24, and 36 forecast horizons are shown for different values of L ranging from 8 to 80. It can be easily seen from this figure that the reconstructed SSA-R forecasting method outperforms SSA-R for the lower values of the window length (L) up to approximately 40. This is in accordance with previous results in simulated series. It is noteworthy that the RRMSE is minimum at $L = 8$ for $h = 1, 3, 6, 12$, and 24. Moreover, the minimum occurs at $L = 12$ when $h = 36$.

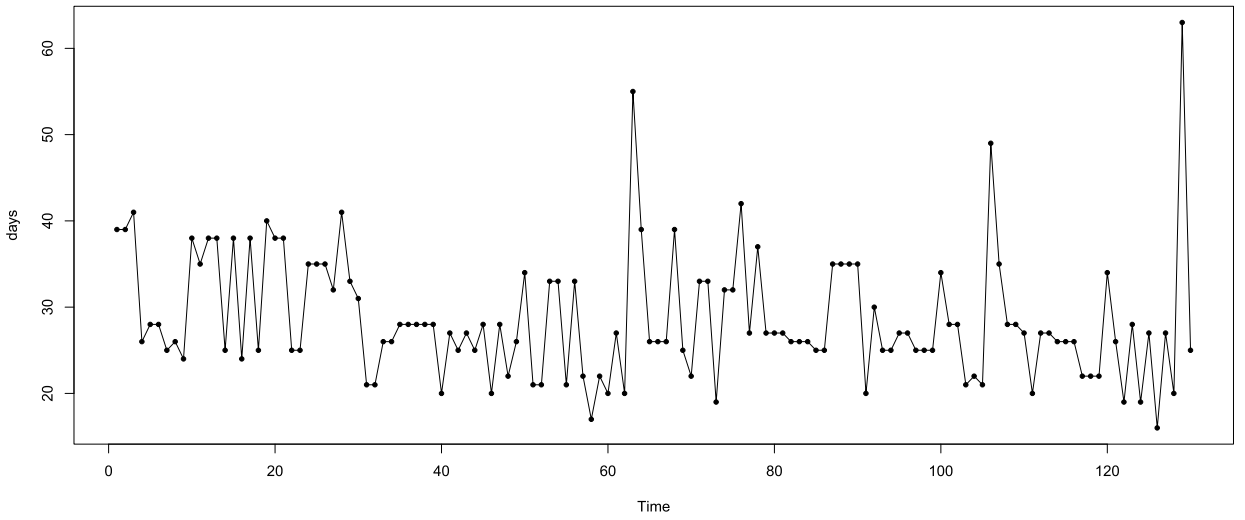

Fig. 7. Time series plot of days series.

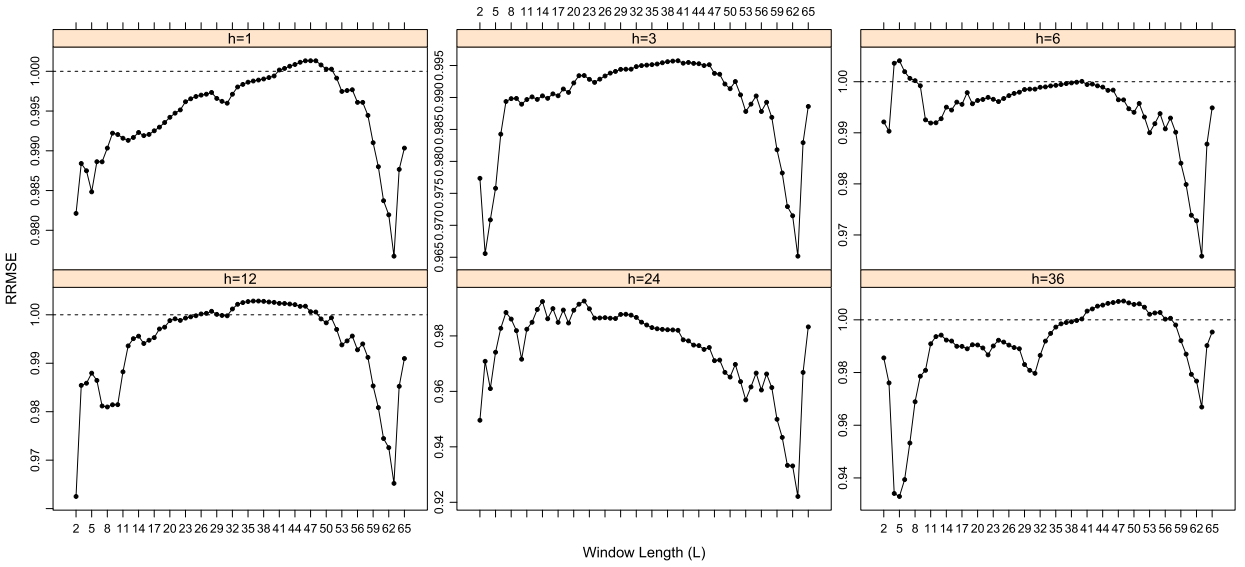

Fig. 8. RRMSE for day series.

Example 4.4. In this example, a time series is considered that contains accounting data from the Winegard Co. of Burlington, Iowa, USA. The data are the number of days until Winegard receives payment for 130 consecutive orders from a particular distributor of Winegard products [7]. Fig. 7 shows the time series plot of these data.

In Fig. 8, the RRMSE for 1, 3, 6, 12, 24, and 36 forecast horizons are depicted for different values of L ranging from 2 to 65. As can be seen from this figure, reconstructed SSA-R forecasting method outperforms SSA-R at forecast horizons 3 and 24. For other values of h, almost always the reconstructed SSA-R forecasting has better performance than the SSA-R method. Note that the RRMSE is minimum at $L = 63, 63, 63, 2, 63$, and 5, corresponding to $h = 1, 3, 6, 12, 24$, and 36.

5. Conclusion

In this paper, we proposed a new forecasting algorithm for univariate time series by improving the recurrent forecasting within the SSA framework. In the proposed method named reconstructed SSA-R, the SSA-R coefficients are generated from the filtered time series as opposed to the basic SSA-R method, whereby the coefficients are generated from the noisy time series. As expected, the new approach will lead to more accurate forecasts.

The performance of the new method was compared with established SSA-R method with respect to the RMSE criteria using both simulated and real world data. The results obtained in this study for various forecasting horizons confirm that

almost always, the reconstructed SSA-R forecasting method outperforms basic SSA-R, especially for lower values of the window length (L).

References

[1] S. Aydin, H.M. Saraoglu, S. Kara, Singular spectrum analysis of sleep EEG in insomnia, J. Med. Syst. 35 (4) (2011) 457–461.
[2] K.L. Bail, J.M. Gipson, D.S. MacMillan, Quantifying the correlation between the MEI and LOD variations by decomposing LOD with singular spectrum analysis, in: Earth on the Edge: Science for a Sustainable Planet, in: International Association of Geodesy Symposia, vol. 139, 2014, pp. 473–477.
[3] D.S. Broomhead, G.P. King, Extracting qualitative dynamics from experimental data, Phys. D, Nonlinear Phenom. 20 (1986) 217–236.
[4] D.S. Broomhead, G.P. King, On the qualitative analysis of experimental dynamical systems, in: S. Sarkar (Ed.), Nonlinear Phenomena and Chaos, Adam Hilger, Bristol, 1986, pp. 113–144.
[5] H-S. Chao, C-H. Loh, Application of singular spectrum analysis to structural monitoring and damage diagnosis of bridges, Struct. Infrastruct. Eng. Maint. Manag. Life-Cycle Des. Perform. 10 (6) (2014) 708–727.
[6] Q. Chen, T.V. Dam, N. Sneeuw, X. Collilieux, M. Weigelt, P. Rebischung, Singular spectrum analysis for modeling seasonal signals from GPS time series, J. Geodyn. 72 (2013) 25–35.
[7] J.D. Cryer, K.S. Chan, Time Series Analysis: With Applications in R, second ed., Springer, 2008.
[8] A.M. De Livera, R.J. Hyndman, R.D. Snyder, Forecasting time series with complex seasonal patterns using exponential smoothing, J. Amer. Stat. Assoc. 106 (496) (2011) 1513–1527.
[9] N. Golyandina, A. Zhigljavsky, Singular Spectrum Analysis for Time Series, Springer Briefs in Statistics, Springer, 2013.
[10] H. Hassani, Singular spectrum analysis: methodology and comparison, J. Data Sci. 5 (2) (2007) 239–257.
[11] H. Hassani, Z. Ghodsi, E.S. Silva, S. Heravi, From nature to maths: improving forecasting performance in subspace-based methods using genetics colonial theory, Digit. Signal Process. 51 (2016) 101–109.
[12] H. Hassani, R. Mahmoudvand, H.N. Omer, E.S. Silva, A preliminary investigation into the effect of outlier(s) on singular spectrum analysis, Fluct. Noise Lett. 13 (14) (2014) 1450029.
[13] H. Hassani, E.S. Silva, N. Antonakakis, G. Filis, R. Gupta, Forecasting accuracy evaluation of tourist arrivals, Ann. Tour. Res. 63 (2017) 112–127.
[14] H. Hassani, A. Webster, E.S. Silva, S. Heravi, Forecasting U.S. tourist arrivals using optimal singular spectrum analysis, Tour. Manag. 46 (2015) 322–335.
[15] Z. Hou, G. Wen, P. Tang, G. Cheng, Periodicity of carbon element distribution along casting direction in continuous-casting billet by using singular spectrum analysis, Metall. Mater. Trans. B 45 (5) (2014) 1817–1826.
[16] R.J. Hydman, Y. Khandakar, Automatic time series forecasting: the forecast package for R, J. Stat. Softw. 27 (3) (2008) 1–22.
[17] R.J. Hyndman, A.B. Koehler, R.D. Snyder, S. Grose, A state space framework for automatic forecasting using exponential smoothing methods, Int. J. Forecast. 18 (3) (2002) 439–454.
[18] K. Liu, S.S. Law, Y. Xia, X.Q. Zhu, Singular spectrum analysis for enhancing the sensitivity in structural damage detection, J. Sound Vib. 333 (2) (2014) 392–417.
[19] B. Muruganatham, M.A. Sanjith, B. Krishnakumar, S.A.V. Satya Murty, Roller element bearing fault diagnosis using singular spectrum analysis, Mech. Syst. Signal Process. 35 (1–2) (2013) 150–166.
[20] S. Sanei, H. Hassani, Singular Spectrum Analysis of Biomedical Signals, Taylor & Francis/CRC, 2016.
[21] E.S. Silva, Z. Ghodsi, M. Ghodsi, S. Heravi, H. Hassani, Cross country relations in European tourist arrivals, Ann. Tour. Res. 63 (2017) 151–168.
[22] E.S. Silva, H. Hassani, On the use of singular spectrum analysis for forecasting U.S. trade before, during and after the 2008 recession, Int. Econ. 141 (2015) 34–49.